Energy 239 (2022) 121923

Contents lists available at ScienceDirect

Energy

journal homepage: www.elsevier.com/locate/energy

A flexible-reliable operation optimization model of the networked energy hubs with distributed generations, energy storage systems and demand response

Anoosh Dini [a], Alireza Hassankashi [a], Sasan Pirouzi [b], Matti Lehtonen [c, *], Behdad Arandian [d], Ali Asghar Baziar [e]

[a] Department of Electrical and Electronics Engineering, Iran University of Science and Technology, Tehran, Iran
[b] Power System Group, Semirom Branch, Islamic Azad University, Semirom, Iran
[c] Department of Electrical Engineering and Automation, Aalto University, Espoo, Finland
[d] Department of Electrical Engineering, Dolatabad Branch, Islamic Azad University, Isfahan, Iran
[e] Department of Electrical Engineering, Missouri University of Science and Technology, Rolla, Missouri, USA

ARTICLE INFO

Article history:
Received 11 February 2021
Received in revised form
20 August 2021
Accepted 26 August 2021
Available online 2 September 2021

Keywords:
Flexible-reliable operation
Flexibility sources
Hybrid evolutionary algorithm
Networked energy hub
Scenario-based stochastic programming

ABSTRACT

This paper presents a novel optimization model for the flexible-reliable operation (FRO) of energy hubs (EHs) in electricity, natural gas, and district heating networks. To achieve flexible EH in the presence of renewable energy sources (RESs) and combined heat and power (CHP) system, energy storage systems (ESS) and incentive-based demand response program (IDRP) are used. The proposed problem minimizes the total expected costs of operation, reliability, and flexibility of the energy networks including EHs. The optimization scheme is constrained to the optimal power flow (OPF) equations and the reliability requirements of these networks and the EH model in the presence of sources and active loads, namely ESS and IDRP. Scenario-based stochastic programming (SBSP) is utilized to model uncertainties of load, energy cost, power generation of RES, and network equipment availability. The problem has a mixed-integer nonlinear programming (MINLP) nature. Consequently, a hybrid teaching-learning-based optimization (TLBO) and crow search algorithm (CSA) is used to obtain a reliable optimal solution with a low standard deviation. Finally, by simulating the proposed scheme on a sample test system, the capabilities of this scheme in improving the reliability, operation, and flexibility of energy networks in accordance with the optimal scheduling for EHs are confirmed.

1. Introduction

Nowadays, with the advancement of new technologies for the generation and storage of environmentally-friendly energy and the interdependence of different energy sources, the use of energy hub (EH) framework to coordinate distributed generations (DGs) and active loads (ALs) has flourished [1]. The most common sources used in EH are renewable energy sources (RESs) due to very low operating costs and pollution emission levels, and combined heat and power (CHP) system thanks to high energy efficiency [2]. It is worth noting that due to the uncertainty in predicting the power generation by RES, the flexibility of EH in the electrical sector will be lower [3]. Moreover, since the heat power of CHP is a function of its active power, the flexibility of EH is low in the heat sector [4]. To compensate for this, the use of flexibility sources (FSs) alongside EHs is suggested, where the energy storage system (ESS) and demand response program (DRP) being the most important FSs to improve the flexibility of a system or EH [5]. Because of the low time constant in these elements, they have a high response speed in changing their operation status [5]. Besides, EHs can provide a significant portion of the energy consumed at the load site due to on-site installation. Thus, it is expected that, due to local energy control in different energy networks, EHs could play an important role in improving the status of technical indices such as operation and reliability, and economic conditions such as their energy consumption costs. Finally, it should be noted that these conditions will

* Corresponding author.
E-mail addresses: a.dini@ieee.org (A. Dini), a_hasankashi@alumni.iust.ac.ir (A. Hassankashi), s.pirouzi@sutech.ac.ir (S. Pirouzi), matti.lehtonen@aalto.fi (M. Lehtonen), b.arandian@yahoo.com (B. Arandian), aliasghar.baziar@yahoo.com (A.A. Baziar).

https://doi.org/10.1016/j.energy.2021.121923

Nomenclature

Indices and sets

e, g, t, h, s, m	Indices of electrical bus, gas node, heat node, hour, scenario, and EH
j	Auxiliary index
ref	Slack bus (node)
$\psi_{EB}, \psi_{GN}, \psi_{TN}, \psi_{H}, \psi_{S}, \psi_{Hub}$	Sets of electrical bus, gas node, heat node, hour, scenario, and EH

Variables

$Cost$	Total expected costs of operation, reliability, and flexibility in energy networks ($)
EE, HE	Electrical energy in the electricity energy storage (EES) and heat energy in the Thermal energy storage (TES) in per unit (p.u.)
$EENS$	Expected energy not-supplied (p.u.)
EFE	Expected flexibility energy (p.u)
ees, tes	Charging/discharging status of the EES and TES
G^{GS}, H^{HS}	Gas power of the natural gas station (p.u.) and heat power of the heat station (p.u.)
G^{L}, H^{L}	Gas and heat power flowing through the distribution pipeline (p.u.)
H^{ch}, H^{dch}	Charging and discharging heat power of the TES (p.u.)
$P^{C}, Q^{C}, G^{C}, H^{C}$	Active, reactive, gas, and heat power of the CHP (p.u.)
P^{ch}, P^{dch}	Charging and discharging active power of the EES (p.u.)
P^{DR}, H^{DR}	Active and heat power in the IDRP (p.u.)
P^{DS}, Q^{DS}	Active and reactive power of the distribution substation (p.u.)
$P^{H}, Q^{H}, G^{H}, H^{H}$	Active, reactive, gas, and heat power of the EH (p.u.)
P^{L}, Q^{L}	Active and reactive power flowing through the distribution line (p.u.)
P^{NS}, G^{NS}, H^{NS}	Active, gas, and heat loads not supplied (p.u.)
V, δ	Voltage magnitude (p.u.) and voltage angle (rad)
ρ, τ	Gas pressure (p.u.) and temperature (p.u.)
γ, μ	Lagrangian multipliers

Constants

A^{E}, A^{G}, A^{H}	Incidence matrices of electrical bus and EH, gas node and EH, and heat node and ES
B, G	Susceptance and conductance of the distribution line (p.u.)
B^{E}, B^{G}, B^{H}	Incidence matrices of electrical bus and distribution line, gas node and gas pipeline, and heat node and heat pipeline
$c\dot{m}$	Specific heat capacity of water and mass flow rate of water through a pipeline
ECR, EDR	Electricity charging and discharging rates of the EES (p.u.)
$\overline{EE}, \underline{EE}, EE^{ini}$	Minimum and maximum storable energy and initial energy of the EES (p.u.)
$\overline{G}^{L}, \overline{G}^{GS}$	Maximum capacity of the pipeline and gas station (p.u.)
HCR, HDR	Heat charging and discharging of the TES (p.u.)
$\overline{HE}, \underline{HE}, HE^{ini}$	Minimum and maximum storable energy and initial energy of the TES (p.u.)
$\overline{H}^{L}, \overline{H}^{HS}$	Maximum capacity of the pipeline and heat station (p.u.)
$P^{D}, Q^{D}, G^{D}, H^{D}$	Active, reactive, gas, and heat load (p.u.)
P^{PV}, P^{W}	Photovoltaic (PV) and wind system (WS) active power (p.u.)
$\overline{S}^{C}, \overline{H}^{C}$	Maximum capacity of the electrical and heat sectors of the CHP (p.u.)
$sign(\rho_g, \rho_j)$	Sign function: equals 1 if $\rho_g > \rho_j$; otherwise, equals -1
$\overline{S}^{L}, \overline{S}^{DS}$	Maximum capacity of the distribution line and substation (p.u.)
$\overline{V}, \underline{V}$	Upper and lower allowable voltage magnitudes (p.u.)
$VOLF$	Value of lost flexibility ($/MWh)
$VOLL$	Value of lost load ($/MWh)
u^{EL}, u^{GL}, u^{HL}	Availability status of distribution line, gas pipeline, and heat pipeline, which has a binary value of 0 or 1
$\lambda^{E}, \lambda^{G}, \lambda^{H}$	Price of electrical, gas, and heat energy ($/MWh)
π	Probability of occurrence of the scenario
κ	Gas pipeline constant (p.u.)
$\overline{\rho}, \underline{\rho}$	Upper and lower allowable gas pressure (p.u.)
$\overline{\tau}, \underline{\tau}$	Upper and lower allowable temperature (p.u.)
$\eta^{EES,ch}, \eta^{EES,dch}$	Charging and discharging efficiency of the EES
$\eta^{T}, \eta^{L}, \eta^{H}$	Efficiency of generator, losses, and heat sector of the CHP
$\eta^{TES,ch}, \eta^{TES,dch}$	Charging and discharging efficiency of the TES
ξ	Participation factor of the consumers in the IDRP

be achieved provided that the energy management system (EMS) is implemented in the mentioned networks and proper coordination is realized between the energy network operators (ENOs) and EH operators (EHOs) [6]. To achieve the mentioned objectives, it is essential to present the optimal energy management problem in energy networks including EHs.

Various researches and studies have already been presented in the field of optimal operation and energy management of EHs. In Ref. [7], the robust operation of EHs consisting of CHP and electric vehicles (EVs) is modeled in electricity, natural gas, and district heating networks. Also, the operating cost of the mentioned networks is limited to optimal power flow (OPF) constraints and the equations governing the mentioned EH. Based on the results of this paper, it can be observed that using EH energy management, operation indices such as energy loss, voltage profile, pressure, and temperature can be improved compared to power flow studies of the mentioned networks. Authors in Ref. [8] examine the optimal participation of EHs in the day-ahead (DA) energy market, where EHs can benefit financially from the energy market by coordinating between different sources and ALs such as ESS, DRP, and EVs. References [9,10] present a definite and robust model of energy management of EHs consisting of RES, ESS, and CHP in electrical, gas, and thermal networks, respectively. Additionally, in these studies, the electrical energy of the hub is supplied through the market with the bilateral contract model and power pool or internal EH resources, but the market model is not provided for other networks. Authors in Refs. [7–10] employ conventional linearization methods to obtain a linear approximation model for the EH operation problem in different networks and then achieve the optimal solution in the shortest possible time using solvers in accordance with linear programming (LP) or mixed-integer LP (MILP). According to Refs. [7–10], the computational error for active and reactive power is roughly 2.5%, 1% for gas power, 0.5% for voltage, and 0.1% for pressure. Its value is more than 10% for power

loss. Therefore, a significant computational error occurs when using linear approximation methods. In Ref. [11], the OPF model of EHs has been modeled in different networks, and a genetic algorithm (GA) is used to solve the problem. Note that the formulation of the energy management problem of energy networks with EHs is nonlinear programming (NLP) or mixed-integer NLP (MINLP) [12]. Therefore, in some studies such as [13–15], evolutionary algorithms (EAs) including time-varying acceleration coefficients particle swarm optimization (TVAC-PSO) algorithm, modified teaching learning-based optimization (MTLBO), and time-varying acceleration coefficient-gravitational search algorithm (TVAC-GSA) are used. The effect of the presence of EHs in the distribution network is investigated in Ref. [16] so that, by proper management of the EH energy network, operation indices such as energy losses and voltage profiles can be improved compared to power flow studies. EH participation in the DRP has also been examined [17] so that, in these conditions, it can achieve peak shaving as another operation index.

A two-stage coordinated volt-pressure optimization (VPO) is proposed [18] for integrated energy systems (IES) that operate in collaboration with energy hubs that contain renewable energy systems. To improve the interdependency of the IES, power-to-gas (P2G) is utilized. The suggested VPO consists of conventional volt-VAR optimization to reduce voltage variations and guarantee desirable gas quality. Besides voltage regulation equipment like on-load tap-changers and capacitor banks, P2G converter and gas storage are also adopted to deal with the voltage fluctuation problem resulting from incorporating renewable energy systems. Aggregated utility curve of multi-energy demands is used to introduce quantitative modeling [19]. To this end, an electricity-shifting curve (ESC) corresponding to the psychology and behavior of the customer is incorporated. Then, utility curves of various types of loads (electricity, heating, and cooling) are merged into a single curve. This curve is used besides the consumer choice theory to depict an ESC considering energy prices. In the end, the paper analyzes the parameters that play a role in the changes in ESCs. Modeling high-efficiency energy hubs is presented [20], although planning multi-energy systems are a time-demanding and overwhelming task. A method is suggested in Ref. [20] to address the available challenges in the planning of energy hubs in an attempt to deal with size limits of devices and multi-scenario problems. Sizes of devices are considered as decision variables. The proposed approach employs a dimension reduction technique and variable-sized unimodal searching (VUS) approach. Energy hubs are scheduled in Ref. [21], in which a concept of virtual energy hub (VEH) is incorporated. The operation of VEH relies on various energy carriers and facilities. The aim of using VEH is to maximize its revenue on the condition it participates in different energy markets. A zoning planning method (ZPM) proposed using the energy hub model is presented to deal with the planning of regional integrated energy system (RIES) [22]. The zoning model of the energy hub is found by investigating the relationship of EHs in terms of energy coupling. Finally, a summary of the literature on the operation of EHs is tabulated in Table 1.

According to the literature review and Table 1, the main research gaps in energy management of EHs are summarized as follows:

- Although the modeling of active loads or flexibility sources such as ESS and DRP in EH has been considered in many studies, their important capability in enhancing the flexibility of EH has rarely been investigated. Following this issue, the mathematical modeling of flexibility in the EH energy management problem has also received less attention. Nonetheless, to determine the flexibility of a system, it is essential to examine the related indices, which can generally be obtained as a mathematical equation.
- In most researches such as [7–22], operation and economic indices are generally considered jointly or individually in EH operation problems. However, the improvement of these indices does not guarantee the enhancement of other indices, such as the reliability and flexibility of energy networks. For instance, to achieve high reliability in a system, it is necessary to consider the high operating cost for that system. Therefore, to simultaneously improve the technical and economic indices of energy networks with EH, these indices are expected to be modeled simultaneously for the operation of these networks.
- As observed based on the literature, the operation of energy networks including EHs is modeled as an NLP or MINLP problem. In some studies, such as [7–10,16,18,20,21], the linear approximation model has been used to solve it, but this method has a significant computational error. Other studies such as [11,13–15] have used single EAs such as GA and PSO. However, to achieve a reliable optimal solution to an optimization problem by EA, a large number of updating steps needs to update the decision variables, which is achievable if the hybrid EA (HEA) is used.

Table 1
Taxonomy of recent research works.

Ref.	Indices				Flexibility model	Problem model	Solver
	Economic	Operation	Flexibility	Reliability			
[7]	✓	✓	✗	✗	✗	LAM	MA
[8]	✓	✓	✗	✗	✗	LAM	MA
[9]	✓	✓	✗	✗	✗	LAM	MA
[10]	✓	✓	✗	✗	✗	LAM	MA
[11]	✓	✓	✗	✗	✗	MINLP	EA
[12]	✓	✓	✗	✗	✗	MINLP	MA
[13]	✓	✓	✗	✗	✗	MINLP	EA
[14]	✓	✓	✗	✗	✗	MINLP	EA
[15]	✓	✓	✗	✗	✗	MINLP	EA
[16]	✓	✓	✗	✗	✗	LAM	MA
[17]	✓	✓	✗	✗	✗	MINLP	MA
[18]	✗	✓	✗	✗	✗	LAM	MA
[19]	✗	✓	✗	✗	✗	Non-linear	MA
[20]	✓	✓	✗	✗	✗	LAM	MA
[21]	✓	✓	✗	✗	✗	LAM	MA
[22]	✓	✓	✗	✗	✗	Non-linear	MA
PS	✓	✓	✓	✓	✓	**MINLP**	**HEA**

PM: Proposed scheme, LAM: Linear approximation model, MA: Mathematical approach, EA: Evolutionary algorithm, HEA: Hybrid EA.

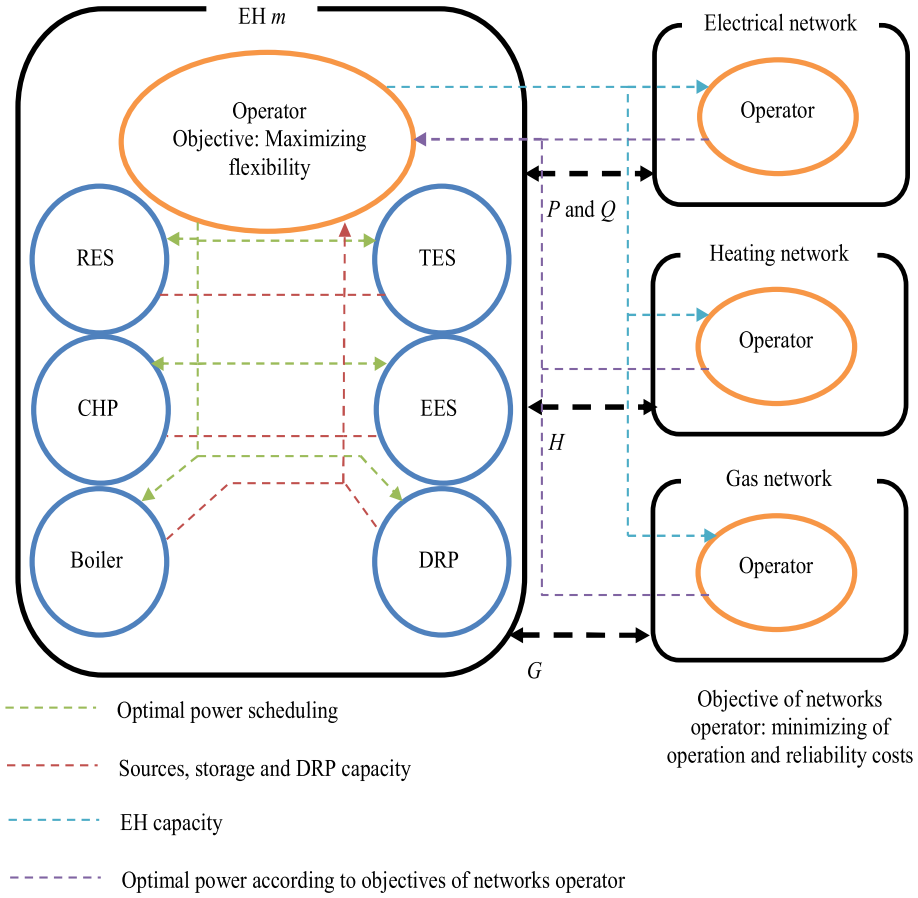

Fig. 1. Proposed scheme hubs operation in different energy networks.

To compensate for the first and second research gaps, this paper as Fig. 1 models the flexible-reliable operation (FRO) of EHs in electricity, natural gas, and district heating networks. In this scheme, EH consists of CHP, electrical energy storage (EES), and incentive-based DRP (IDRP) to improve its flexibility in the electrical sector in the presence of RES. It also uses thermal energy storage (TES) and IDRP in the thermal sector to improve its flexibility in the presence of CHP. Concerning the second research gap, the proposed problem is to minimize the total expected costs of operation, reliability, and flexibility of these networks. The problem has also OPF constraints constrained to reliability for the mentioned networks, and EH formulation in the presence of the mentioned sources and ALs. Furthermore, the proposed scheme is constrained to uncertainties in load, energy cost, RES generation power, and network equipment availability. Thus, scenario-based stochastic programming (SBSP) is used to model these uncertain parameters. The method uses the roulette wheel mechanism (RWM) to generate a large number of scenarios. Then, the Kantorovich method, as a scenario reduction technique, selects a certain number of scenarios that are likely to occur. To bridge the third research gap, this paper uses a HEA that combines teaching-learning-based optimization (TLBO) and crow search algorithm (CSA). Since the suggested EA has a combination of three update steps, i.e. the teacher phase, the student phase, and the CSA, for the decision variables, it is predicted that it will be able to achieve a reliable optimal solution with a low standard deviation in response. Finally, the contributions of the proposed scheme can be summarized as follows:

- Modeling flexible-reliable operation in electricity, natural gas, and district heating networks by taking into account the presence of EHs,
- Simultaneous formulation of operation, reliability, flexibility, and economic indices for the energy management problem of EHs in energy networks,
- Use of ESS and IDRP to improve EH flexibility in the presence of RES and CHP,
- Solving the FRO problem of energy networks with EH using the hybrid TLBO-CSA to achieve an optimal, reliable solution with a low standard deviation in the response.

The paper is organized as follows: Section 2 describes the formulation of the energy management problem of EHs in different energy networks. In Section 3, the problem-solving process is presented in accordance with the hybrid TLBO and CSA. In the end, the numerical results are evaluated in Section 4, and finally, conclusions are given in Section 5 of the paper.

2. Problem formulation

This section describes the mathematical model of the FRO problem of EHs in electricity, natural gas, and district heating networks. This minimizes the expected costs of operation, reliability, and flexibility of energy networks. It is also constrained to OPF equations and the reliability constraints of these networks and EH formulation. Therefore, the model of the proposed scheme problem will be as follows:

$$\min \ \text{Cost} = \sum_{s\in\Psi_S}\pi_s \sum_{h\in\Psi_H}\left\{\lambda^E_{h,s}P^{DS}_{ref,h,s}+\lambda^G_{h,s}G^{GS}_{ref,h,s}+\lambda^H_{h,s}H^{HS}_{ref,h,s}\right\}+ \overbrace{VOLL.\sum_{s\in\Psi_S}\pi_s\sum_{h\in\Psi_H}\left\{\sum_{e\in\Psi_{EB}}P^{NS}_{e,h,s}+\sum_{g\in\Psi_{GN}}G^{NS}_{e,h,s}+\sum_{t\in\Psi_{TN}}H^{NS}_{e,h,s}\right\}}+ \overbrace{VOLF.\sum_{s\in\Psi_S}\pi_s\sum_{h\in\Psi_H}\sum_{m\in\Psi_{Hub}}\left\{\left|P^H_{m,h,s}-P^H_{m,h,s=1}\right|+\left|H^H_{m,h,s}-H^H_{m,h,s=1}\right|\right\}} \quad (1)$$

Subject to:

$$P^{NS}_{e,h,s}+P^{DS}_{e,h,s}-P^{D}_{e,h,s}+\sum_{m\in\Psi_{Hub}}A^E_{e,m}P^H_{m,h,s}=\sum_{j\in\Psi_{EB}}B^E_{e,j}P^L_{e,j,h,s}\quad \forall e,h,s \quad (2)$$

$$Q^{DS}_{e,h,s}-Q^{D}_{e,h,s}+\sum_{m\in\Psi_{Hub}}A^E_{e,m}Q^H_{m,h,s}=\sum_{j\in\Psi_{EB}}B^E_{e,j}Q^L_{e,j,h,s}\quad \forall e,h,s \quad (3)$$

$$P^L_{e,j,h,s}=\left\{G_{e,j}(V_{e,h,s})^2-V_{e,h,s}V_{j,h,s}\left\{G_{e,j}\cos\left(\delta_{e,h,s}-\delta_{j,h,s}\right)+B_{e,j}\sin\left(\delta_{e,h,s}-\delta_{j,h,s}\right)\right\}\right\}u^{EL}_{e,j,h,s}\ \forall e,j,h,s \quad (4)$$

$$Q^L_{e,j,h,s}=\left\{-B_{e,j}(V_{e,h,s})^2+V_{e,h,s}V_{j,h,s}\left\{B_{e,j}\cos\left(\delta_{e,h,s}-\delta_{j,h,s}\right)-G_{e,j}\sin\left(\delta_{e,h,s}-\delta_{j,h,s}\right)\right\}\right\}u^{EL}_{e,j,h,s}\ \forall e,j,h,s \quad (5)$$

$$\delta_{e,h,s}=0\quad \forall e=\text{Slack bus},h,s \quad (6)$$

$$G^{NS}_{g,h,s}+G^{GS}_{g,h,s}-G^{D}_{g,h,s}+\sum_{m\in\Psi_{Hub}}A^G_{g,m}G^H_{m,h,s}=\sum_{j\in\Psi_{GN}}B^G_{g,j}G^L_{g,j,h,s}\quad \forall g,h,s \quad (7)$$

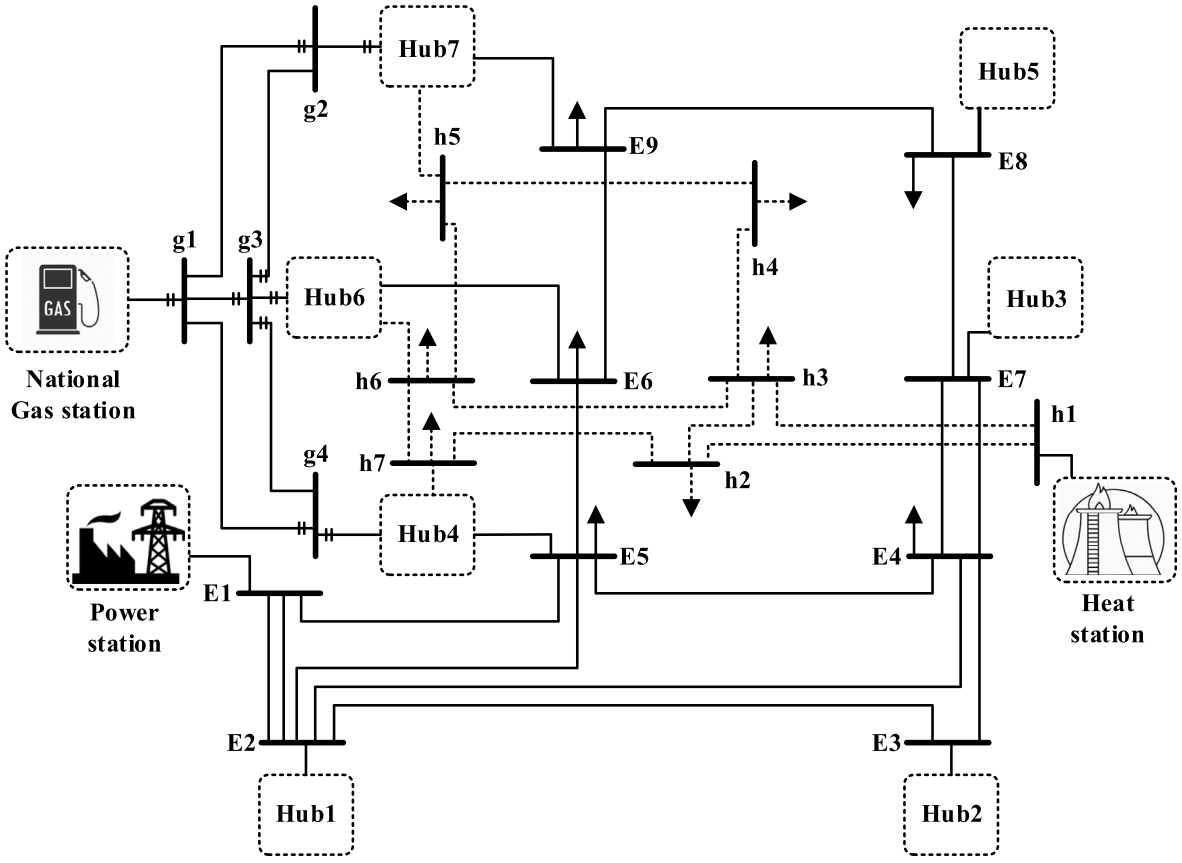

Fig. 2. Test system [8].

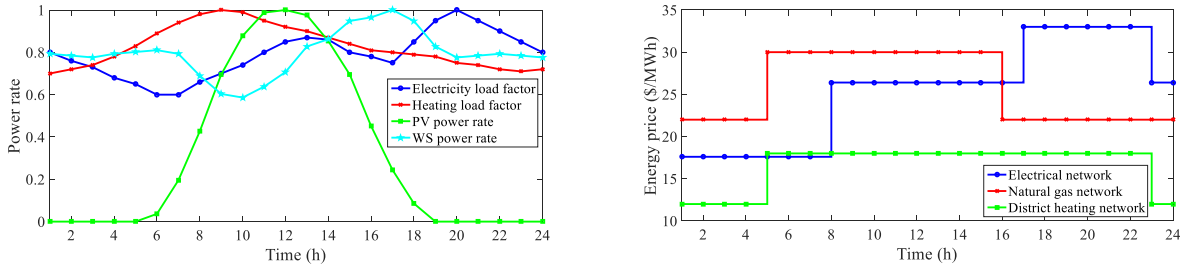

(a) (b)

Fig. 3. Daily curve of, a) load factor [8] and RES power rate [40], b) energy price [8].

Table 2
Hub characterizes (in p.u) [7–10].

Hub	ξ (%)	PV capacity	WS capacity	Electrical/thermal capacity of CHP	EES			TES		
					$\underline{EE}/\overline{EE}/EE^{ini}$	ECR/EDR	η^{ch}/η^{dch} (%)	$\underline{HE}/\overline{HE}/HE^{ini}$	HCR/HDR	η^{ch}/η^{dch} (%)
1	30	0.25	0.2		0.1/2.2/0.1	0.3/0.3	0.93/0.93			
2	30	0.25	0.2		0.1/2.2/0.1	0.3/0.3	0.93/0.93			
3	30	0.25	0.2		0.1/2.2/0.1	0.3/0.3	0.93/0.93			
4	30			1/1				0.1/2/2	0.3/0.3	0.80/0.80
5	30	0.25	0.2		0.1/2.2/0.1	0.3/0.3	0.93/0.93			
6	30	0.25	0.2	1/1	0.1/2.2/0.1	0.3/0.3	0.93/0.93	0.1/2/2	0.3/0.3	0.80/0.80
7	30	0.25	0.2	1/1	0.1/2.2/0.1	0.3/0.3	0.93/0.93	0.1/2/2	0.3/0.3	0.80/0.80

$$G^{L}_{g,j,h,s} = u^{GL}_{g,j,h,s} K_{g,j} sign\left(\rho_{g,h,s}, \rho_{j,h,s}\right) \sqrt{sign\left(\rho_{g,h,s}, \rho_{j,h,s}\right)\left(\rho^{2}_{g,h,s} - \rho^{2}_{j,h,s}\right)} \quad \forall g,j,h,s \tag{8}$$

$$H^{NS}_{t,h,s} + H^{HS}_{t,h,s} - H^{D}_{t,h,s} + \sum_{m \in \Psi_{Hub}} A^{H}_{t,m} H^{H}_{m,h,s} = \sum_{j \in \Psi_{TN}} B^{H}_{t,j} H^{L}_{h,j,h,s} \quad \forall t,h,s \tag{9}$$

$$H^{L}_{t,j,h,s} = u^{HL}_{t,j,h,s} c_{t,j} \dot{m}_{t,j}\left(\tau_{t,h,s} - \tau_{j,h,s}\right) \quad \forall t,j,h,s \tag{10}$$

$$\underline{V}_{e} \le V_{e,h,s} \le \overline{V}_{e} \quad \forall e,h,s \tag{11}$$

$$\sqrt{\left(P^{L}_{e,j,h,s}\right)^{2} + \left(Q^{L}_{e,j,h,s}\right)^{2}} \le \overline{S}^{L}_{e,j} \quad \forall e,j,h,s \tag{12}$$

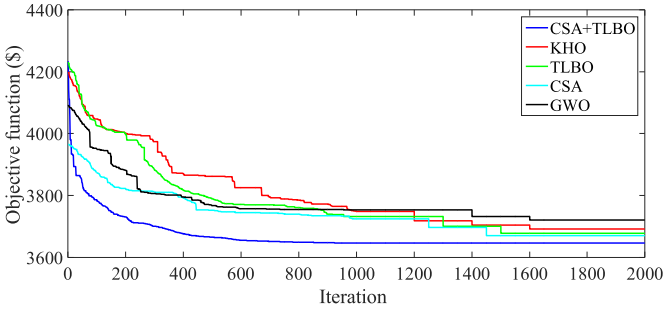

Fig. 4. Convergence curve of different solvers for the proposed problem.

Table 3
Results of different algorithms.

Algorithm	Objective function value ($)	Standard deviation (%)	Convergence iteration	Calculation time (sec)
BARON	3685.4	0.93	184	972.4
BONMIN	3665.2	0.92	143	811.4
DISOPT	Infeasible solution			
KNITRO	Infeasible solution			
GWO	3721.3	2.13	1612	350.7
KHO	3692.5	1.78	1601	354.1
TLBO	3678.2	1.41	1508	310.5
CSA	3670.1	1.34	1452	301.2
TLBO + CSA	3646.4	0.91	990	237.3

$$\sqrt{\left(P_{e,h,s}^{DS}\right)^2+\left(Q_{e,h,s}^{DS}\right)^2}\le \overline{S}_e^{DS} \quad \forall e,h,s \tag{13}$$

$$\underline{\rho}_g \le \rho_{g,h,s} \le \overline{\rho}_g \quad \forall g,h,s \tag{14}$$

$$-\overline{G}_{g,j}^{L} \le G_{g,j,h,s}^{L} \le \overline{G}_{g,j}^{L} \quad \forall g,j,h,s \tag{15}$$

$$-\overline{G}_{g}^{GS} \le G_{g,h,s}^{GS} \le \overline{G}_{g}^{GS} \quad \forall g,h,s \tag{16}$$

$$\underline{\tau}_t \le \tau_{t,h,s} \le \overline{\tau}_t \quad \forall t,h,s \tag{17}$$

$$-\overline{H}_{t,j}^{L} \le H_{t,j,h,s}^{L} \le \overline{H}_{t,j}^{L} \quad \forall t,j,h,s \tag{18}$$

$$-\overline{H}_{t}^{HS} \le H_{t,h,s}^{HS} \le \overline{H}_{t}^{HS} \quad \forall t,h,s \tag{19}$$

$$0 \le P_{e,h,s}^{NS} \le P_{e,h,s}^{D} \quad \forall e,h,s \tag{20}$$

$$0 \le G_{g,h,s}^{NS} \le G_{g,h,s}^{D} \quad \forall g,h,s \tag{21}$$

$$0 \le H_{t,h,s}^{NS} \le H_{t,h,s}^{D} \quad \forall t,h,s \tag{22}$$

$$P_{m,h,s}^{H} = P_{m,h,s}^{C} + P_{m,h,s}^{PV} + P_{m,h,s}^{W} + \left(P_{m,h,s}^{dch} - P_{m,h,s}^{ch}\right) + P_{m,h,s}^{DR} - P_{m,h,s}^{D} \quad \forall m,h,s \tag{23}$$

$$Q_{m,h,s}^{H} = Q_{m,h,s}^{C} - Q_{m,h,s}^{D} \quad \forall m,h,s \tag{24}$$

$$G_{m,h,s}^{H} = -G_{m,h,s}^{C} \quad \forall m,h,s \tag{25}$$

$$H_{m,h,s}^{H} = H_{m,h,s}^{C} + \left(H_{m,h,s}^{dch} - H_{m,h,s}^{ch}\right) + H_{m,h,s}^{DR} - H_{m,h,s}^{D} \quad \forall m,h,s \tag{26}$$

$$H_{m,h,s}^{C} = \frac{P_{m,h,s}^{C}\left(1-\eta_m^T-\eta_m^L\right)}{\eta_m^T}\eta_m^H \quad \forall m,h,s \tag{27}$$

$$G_{m,h,s}^{C} = \frac{P_{m,h,s}^{C}}{\eta_m^T} \quad \forall m,h,s \tag{28}$$

$$\sqrt{\left(P_{m,h,s}^{C}\right)^2+\left(Q_{m,h,s}^{C}\right)^2} \le \overline{S}_m^{C} \quad \forall m,h,s \tag{29}$$

$$0 \le H_{m,h,s}^{C} \le \overline{H}_m^{C} \quad \forall m,h,s \tag{30}$$

$$HE_{m,h+1,s} = HE_{m,h,s} + \eta^{TES,ch}H_{m,h,s}^{ch} - \frac{1}{\eta^{TES,dch}}H_{m,h,s}^{dch} \quad \forall m,h,s \tag{31}$$

$$0 \le H_{m,h,s}^{ch} \le HCR_m tes_{m,h} \quad \forall m,h,s \tag{32}$$

$$0 \le H_{m,h,s}^{dch} \le HDR_m\left(1-tes_{m,h}\right) \quad \forall m,h,s \tag{33}$$

$$HE_{m,h,s} = HE_{m}^{ini} \quad \forall m,h=1,s \tag{34}$$

$$\underline{HE}_m \le HE_{m,h,s} \le \overline{HE}_m \quad \forall m,h,s \tag{35}$$

$$EE_{m,h+1,s} = EE_{m,h,s} + \eta^{EES,ch}P_{m,h,s}^{ch} - \frac{1}{\eta^{EES,dch}}P_{m,h,s}^{dch} \quad \forall m,h,s \tag{36}$$

$$0 \le P_{m,h,s}^{ch} \le ECR_m ees_{m,h} \quad \forall m,h,s \tag{37}$$

$$0 \le P_{m,h,s}^{dch} \le EDR_m\left(1-ees_{m,h}\right) \quad \forall m,h,s \tag{38}$$

$$EE_{m,h,s} = EE_{m}^{ini} \quad \forall m,h=1,s \tag{39}$$

$$\underline{EE}_m \le EE_{m,h,s} \le \overline{EE}_m \quad \forall m,h,s \tag{40}$$

$$-\xi.P_{m,h,s}^{D} \le P_{m,h,s}^{DR} \le \xi.P_{m,h,s}^{D} \quad \forall m,h,s \tag{41}$$

$$\sum_{h\in\Psi_H} P_{m,h,s}^{DR} = 0 \quad \forall m,s \tag{42}$$

$$-\xi.H_{m,h,s}^{D} \le H_{m,h,s}^{DR} \le \xi.H_{m,h,s}^{D} \quad \forall m,h,s \tag{43}$$

$$\sum_{h\in\Psi_H} H_{m,h,s}^{DR} = 0 \quad \forall m,s \tag{44}$$

A) *Objective function*: Eq. (1) represents the objective function of the proposed problem, which has three terms. The first term refers to the total expected operating costs of electricity, natural gas, and district heating networks [8]. Also, the second term denotes the expected reliability cost of the mentioned networks. In this paper, the reliability cost is equal to the shutdown cost [23], in other words, it is equal to the product of the value of lost load (VOLL) and the expected energy not-supplied (EENS) [23]. The EENS also includes the total energy not-supplied in electricity, natural gas, and district heating networks. Furthermore, in the third term of Eq. (1), the expected flexibility cost of energy networks is modeled. In this paper, the only source in the energy networks is the EH, so achieving a flexible EH ensures the high flexibility of these networks. Hence, the third term of Eq. (1) presents the expected flexibility cost for all EHs. In this regard, the cost is proportional to the product of the value of lost flexibility (VOLF) and expected flexibility energy (EFE) [3]. Note that in the electrical (heat) part of the EH, RES (CHPs) reduce the flexibility of the EH, and there are no such conditions in the gas sector. So, EFE is then considered for the electrical and heating parts of the EH according to Eq. (1). Another point is that flexibility is defined as "*correcting the generation injection and/or consumption pathways in a reaction to an external price or activation signal to provide a service in an electrical system*" [3]. Therefore, to improve the flexibility of the system, the difference between the active (heating) power in scenario *s* and the scenario corresponding to the deterministic model (scenario 1 considers for this case) should be minimal, where zero value means high flexibility of the system [3].

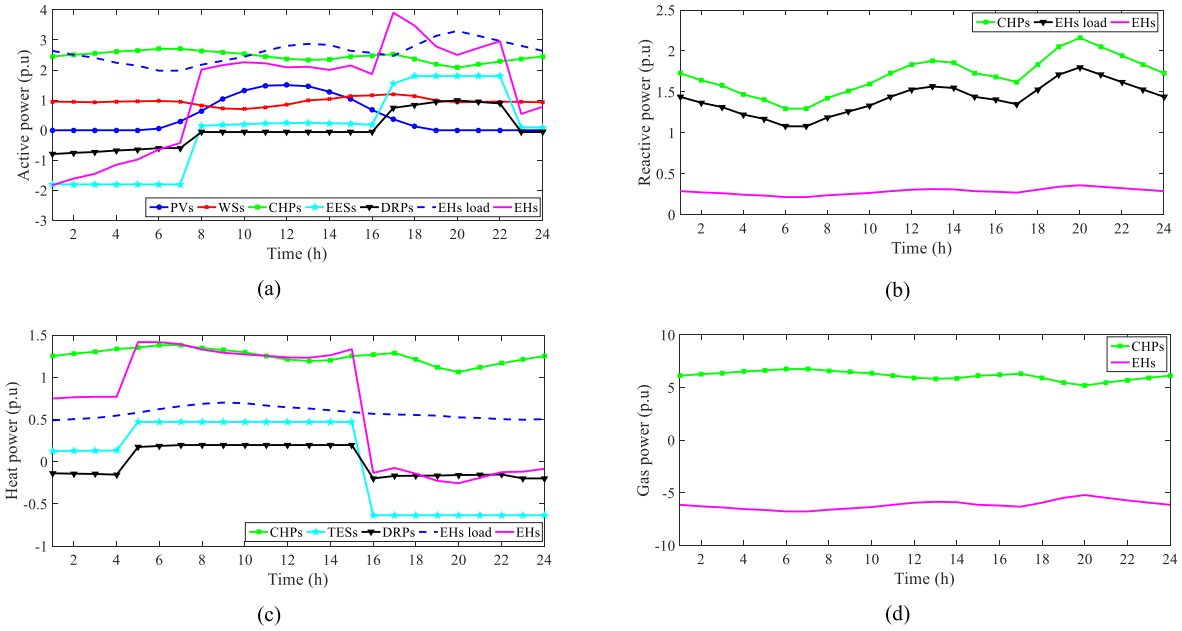

Fig. 5. Expected daily curve of, a) active power, b) reactive power, c) heat power, d) gas power of EHs and EH devices.

B) *Constraints of energy networks*: These constraints include the OPF equations constrained to reliability in electricity, natural gas, and district heating networks in the form of Eqs. (2)–(22). Eqs. (2)–(10) are related to the power flow (PF) constraints of these networks [7,8]. Eqs. (2)–(6) are equal to the PF model in the electrical network, which represents the nodal active and reactive power balance, active and reactive power flowing through the distribution lines, and the slack bus voltage [24–26]. Also, the PF model of the natural gas network is in accordance with the constraints (7) and (8) [7], which refer to the balance of gas power in the nodes and the amount of gas power flowing through the distribution pipeline, respectively. Eqs. (9) and (10) represent the formulation of PF in the district heating network, so that constraint (9) represents the balance of heat power in the nodes and constraint (10) is related to the computational equation of heat power flowing through a distribution pipeline [8]. It is noteworthy that in these equations, P^{DS}, Q^{DS}, G^{GS}, and H^{HS} are proportional to the power of electrical, gas, and heat stations, which are assumed to be connected to the slack bus (node). Therefore, these variables have a value only in the slack bus (node) and are zero in the other nodes. The parameters u^{EL}, u^{GL} and u^{HL} also indicate the availability of distribution lines or pipelines in the event of an internal fault in the equipment. In other words, if the values of these parameters are equal to 1, the mentioned devices are present in the power grids; otherwise, the parameters are assumed to be zero. Besides, the technical limitations of electric, natural gas, and district heating networks are presented in (11)–(13) [27–29], (14)–(16) and (17)–(19) [7–10], respectively. In each part, these equations represent the limits on bus voltages (pressure or temperature of the nodes), the power flow limitation of the distribution lines (gas or heat pipelines), and the capacity limit of the distribution substation (gas or heating station), respectively. Finally, the reliability constraints of energy networks are formulated in Eqs. (20)–(22), each of which refers to the range of load not-supplied (LNS) in these networks.

C) *Constraints of EH*: The equations concerning the EH are given in Eqs. (23)–(44), where constraints (23)–(26) refer to the balance of active, reactive, gas, and heat power, respectively, between FSs and non-FSs. In this paper, FS in the electrical sector of EH includes DRP, EES, and CHP, while in the heating sector of EH it has TES and DRP. Moreover, RESs in the electrical sector and CHPs in the heating sector will be non-FS. Next, the CHP constraints are given by (27)-(30) [7], in which the heat and gas power of the CHP are calculated based on (27) and (28), respectively. Also, the CHP output capacity limits in the electrical and heating sectors are expressed in constraints (29) and (30), respectively. In addition, Eqs. (31)–(35) represent the TES model, which provides the energy stored in the TES, (31), the heat charging and discharging rate limits, (32) and (33), the initial energy of TES, (34), and the energy limit of TES, (35). The same equations apply to EES, which are expressed in (36)-(40) [30,31], except that electrical energy and active power are used in these equations. Finally, DRP modelings in electrical and heating networks are expressed in (41)-(42) and (43)-(44), respectively [5,23]. The scheme is based on an incentive model, which assumes that responsive loads can reduce consumption during high energy price hours. They are also able to receive this unused energy from the grid during low energy price hours. Therefore, it is expected that the loads, according to the proposed DRP plan, will shift part of their consumption during peak hours (corresponding to high energy price) to off-peak hours (proportional to low energy price). Thus, constraints (41) and (43) are related to the limitation of DRP power changes, and constraints (42) and (44) ensure that the total energy not consumed during peak hours is received from the grid during off-peak hours.

D) *SBSP model*: In the proposed problem, parameters such as load, P^D, Q^D, G^D and H^D, energy price, λ^E, λ^G, and λ^H, RES power, P^{PV}, and P^W, and availability of power network equipment, u^{EL}, u^{GL}, and u^{HL} are uncertain. Based on Eq. (1), different renewable power generation scenarios need to be analyzes to calculate flexibility indices such as flexibility cost presented in the third term of Eq. (1). Also, to accurately

Table 4
Economic and operation results.

Economic results				
Case	Expected energy cost ($) in the network of			Total expected energy cost ($)
	Electrical	Natural gas	District heating	
I	2081.8	0	2241	4323.8
II	1098.8	1425.4	1122.2	3646.4
Operation results				
Case	Expected energy loss (p.u) in the network of			Total expected energy loss (p.u)
	Electrical	Natural gas	District heating	
I	2.3284	0	2.5036	4.832
II	1.4109	1.1381	1.5200	4.069
Case	Max voltage drop (p.u)	Max pressure drop (p.u)	Max temperature drop (p.u)	Feasible condition
I	0.157	0	0.195	No
II	0.097	0.063	0.029	Yes
Case	Max over-voltage (p.u)	Max over-pressure (p.u)	Max over-temperature (p.u)	Feasible condition
I	0	0	0	Yes
II	0	0	0.012	Yes

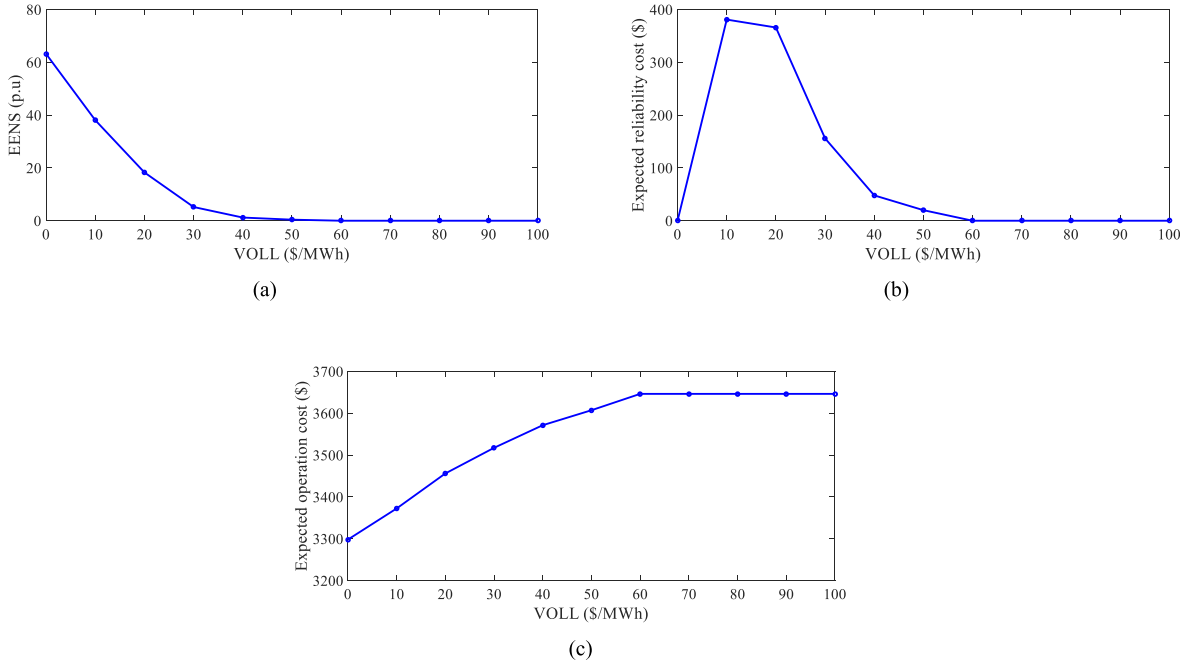

Fig. 6. Curve of, a) EENS, b) reliability cost, c) operation cost in VOLL.

calculate the reliability index as given in Ref. [23], different N - 1 events should be investigated, meaning that different cases of u^{EL}, u^{GL}, and u^{HL} need to be examined. Hence, different scenarios are considered to the provided uncertainties. This part of the paper uses SBSP to model the mentioned uncertainty. Initially, the RWM generates a large number of scenarios, in which, the probability of load and energy prices is calculated from the normal probability distribution function (PDF) in each scenario [32]. The probability values of P^{PV}, P^{W}, and equipment availability in each scenario are also calculated from beta, Weibull, and Bernoulli PDFs, respectively [33,34]. Bernoulli PDF also determines the probability of u^{EL}, u^{GL}, and u^{HL} values according to the forced outage rate (FOR) of the equipment [33]. Then, the Kantorovich method is used as a scenario reduction method to determine a certain number of scenarios produced with a high probability of occurrence [35].

3. Solution method

The proposed problem described by the model given in (1)-(44) is MINLP. To cope with the third research gap in Section 1, the priority of the solver is HEA. So, to achieve an optimal reliable solution, a combination of TLBO [36] and CSA [37] (called TLBO + CSA) is utilized in this study. Note that if the number of steps to update decision variables in EAs is high, the probability of obtaining a reliable optimal point with a low standard deviation in the response will be high. Since the proposed algorithm has three stages of updating the decision variables, namely the teacher phase, the student phase, and the CSA, it is expected that the achievement of this goal is certain. For example, results obtained from GA with the mutation process are more favourable than GA without the mutation process [38]. This is because when the mutation process is added to the GA, the decision variables in the two general processes, the primary GA process and the mutation process, are

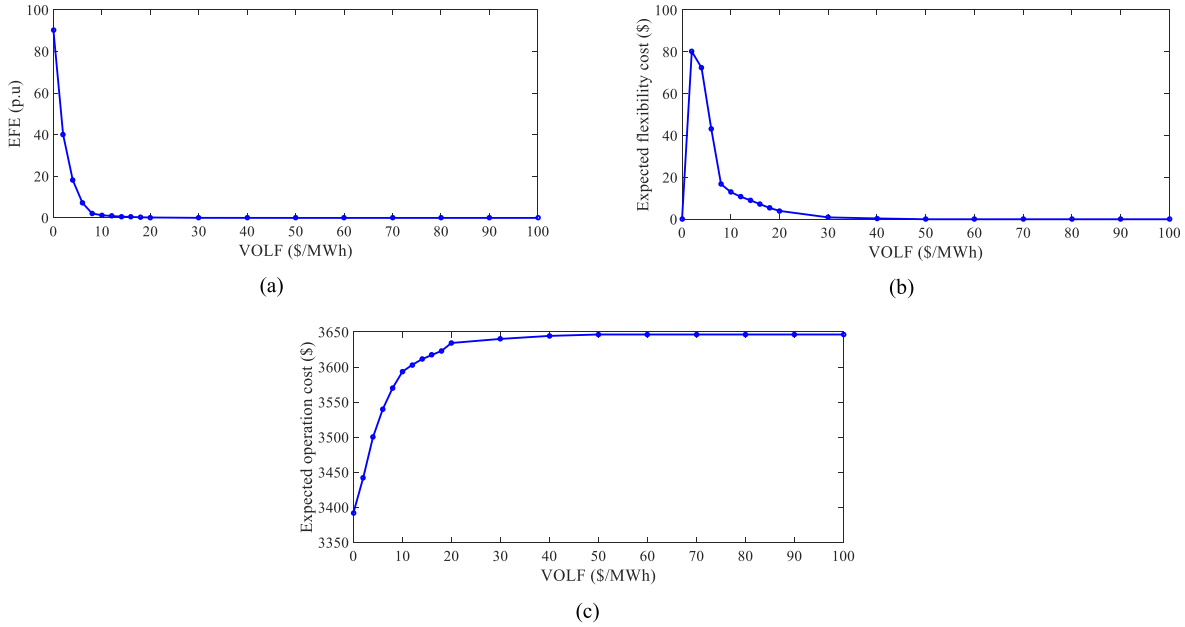

Fig. 7. The curve of, a) EFE, b) flexibility cost, c) operation cost in VOLF.

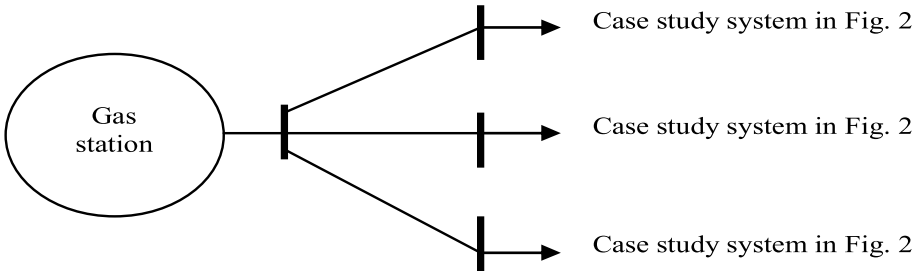

Fig. 8. A large scale case study system.

updated differently. Therefore, the optimal point obtained from GA with the mutation process is more desirable than GA without the mutation process. Note that the capabilities of the mentioned solver are reported in subsection 4.2.A. In addition, in solving problems by the EA, the problem should be in the standard format in accordance with the EA, which is given in (45)-(58). In this format, problem variables are divided into two categories: decision variables and dependent variables. The decision variables in the

Table 5
Convergence, economic and technical results.

Convergence results				
Algorithm	Objective function value ($)	Standard deviation (%)	Convergence iteration	Calculation time (sec)
BONMIN	11011.4	0.95	281	1602.7
TLBO	11055.8	2.53	2932	595.5
CSA	11032.2	2.22	2811	578.3
TLBO + CSA	10951.6	0.92	1651	456.2
Economic results				
Case		I		II
Total expected energy cost ($)		13052.7		10951.6
Technical results				
Case		I		II
Total expected energy loss (p.u)		14.522		12.310
Max voltage drop (p.u)		0.157		0.097
Max pressure drop (p.u)		0		0.065
Max temperature drop (p.u)		0.195		0.029
Max over-voltage (p.u)		0		0
Max over-pressure (p.u)		0		0
Max over-temperature (p.u)		0		0.012
EFE with considering VOLF = 100 $/MWh		–		0
EENS with considering VOLL = 100 $/MWh		185.3		0

proposed problem include P^{NS}, G^{NS}, H^{NS}, P^{C}, Q^{C}, H^{ch}, H^{dch}, tes, P^{ch}, P^{dch}, ees, P^{DR}, and H^{DR}, and the rest are dependent variables. In the new problem, the objective function, as given in (45), is the sum of the objective function of the main problem (1) and the penalty function of equality and inequality constraints [39]. The penalty function for the constraint $a \le b$ will be $\mu.\max(0, a-b)$, where $\mu \ge 0$ represents the Lagrangian multipliers. For the constraint $a - b = 0$, it is also expressed as $\gamma.(a-b)$, where $\gamma \in (-\infty, +\infty)$ denotes the Lagrange multipliers [39]. Lagrange multipliers in the new problem, (45)–(58) are considered as decision variables. Noted that the penalty function is used for constraints in which the variables were calculated from other equations. For example, in the proposed scheme, the dependent variables are calculated from constraint (46), which include PF equations 2–10, the power balance in EH (23)–(26), gas and heat power calculations of the CHP (27)–(28), and energy calculations of EES and TES (31), (34), (36), and (39). Decision variables are also determined by constraints (47)–(58) by the TLBO + CSA. Thus, constraints (11)–(19), (29), (30), (35), (40), (42) and (44) appear as a penalty function in the objective function. At the optimal point, the values of the penalty function are expected to be zero, which means satisfying the above constraints. Also, in this paper, the Newton-Raphson method is utilized to solve constraint (46).

$$\min \quad \text{Cost} + \sum_{e,h,s}\left\{\begin{array}{l}\overline{\mu}^{v}_{e,h,s}.\max\left(0, V_{e,h,s}-\overline{V}_{e}\right)+\underline{\mu}^{v}_{e,h,s}.\max\left(0, \underline{V}_{e}-V_{e,h,s}\right)+\overline{\mu}^{ds}_{e,h,s}.\max\left(0, \sqrt{\left(P^{DS}_{e,h,s}\right)^2+\left(Q^{DS}_{e,h,s}\right)^2}-\overline{S}^{DS}_{e}\right)\\ +\sum_{j}\overline{\mu}^{el}_{e,j,h,s}.\max\left(0, \sqrt{\left(P^{L}_{e,j,h,s}\right)^2+\left(Q^{L}_{e,j,h,s}\right)^2}-\overline{S}^{L}_{e,j}\right)\end{array}\right\}+$$

$$\sum_{g,h,s}\left\{\begin{array}{l}\overline{\mu}^{\rho}_{g,h,s}.\max\left(0, \rho_{g,h,s}-\overline{\rho}_{g}\right)+\underline{\mu}^{\rho}_{g,h,s}.\max\left(0, \underline{\rho}_{g}-\rho_{g,h,s}\right)+\overline{\mu}^{gs}_{g,h,s}.\max\left(0, G^{GS}_{g,h,s}-\overline{G}^{GS}_{g}\right)+\\ \underline{\mu}^{gs}_{g,h,s}.\max\left(0, -\overline{G}^{GS}_{g}-G^{GS}_{g,h,s}\right)+\sum_{j}\left(\overline{\mu}^{gl}_{g,j,h,s}.\max\left(0, G^{L}_{g,j,h,s}-\overline{G}^{L}_{g,j}\right)+\underline{\mu}^{gl}_{g,j,h,s}.\max\left(0, -\overline{G}^{L}_{g,j}-G^{L}_{g,j,h,s}\right)\right)\end{array}\right\}+$$

$$\sum_{t,h,s}\left\{\begin{array}{l}\overline{\mu}^{\tau}_{t,h,s}.\max\left(0, \tau_{t,h,s}-\overline{\tau}_{t}\right)+\underline{\mu}^{\tau}_{t,h,s}.\max\left(0, \underline{\tau}_{t}-\tau_{t,h,s}\right)+\overline{\mu}^{hs}_{t,h,s}.\max\left(0, H^{HS}_{t,h,s}-\overline{H}^{HS}_{t}\right)+\\ \underline{\mu}^{hs}_{t,h,s}.\max\left(0, -\overline{H}^{HS}_{t}-H^{HS}_{t,h,s}\right)+\sum_{j}\left(\overline{\mu}^{hl}_{t,j,h,s}.\max\left(0, H^{L}_{t,j,h,s}-\overline{H}^{L}_{t,j}\right)+\underline{\mu}^{hl}_{t,j,h,s}.\max\left(0, -\overline{H}^{L}_{t,j}-H^{L}_{t,j,h,s}\right)\right)\end{array}\right\}+ \tag{45}$$

$$\sum_{m,h,s}\left\{\begin{array}{l}\overline{\mu}^{sc}_{m,h,s}.\max\left(0, \sqrt{\left(P^{C}_{m,h,s}\right)^2+\left(Q^{C}_{m,h,s}\right)^2}-\overline{S}^{C}_{m}t\right)+\overline{\mu}^{hc}_{m,h,s}.\max\left(0, H^{C}_{m,h,s}-\overline{H}^{C}_{m}\right)+\underline{\mu}^{hc}_{m,h,s}.\max\left(0, -H^{C}_{m,h,s}\right)+\\ \overline{\mu}^{he}_{m,h,s}.\max\left(0, HE_{m,h,s}-\overline{HE}_{m}\right)+\underline{\mu}^{he}_{m,h,s}.\max\left(0, \underline{HE}_{m}-HE_{m,h,s}\right)+\overline{\mu}^{ee}_{m,h,s}.\max\left(0, EE_{m,h,s}-\overline{EE}_{m}\right)+\\ \underline{\mu}^{ee}_{m,h,s}.\max\left(0, \underline{EE}_{m}-EE_{m,h,s}\right)\end{array}\right\}+$$

$$\sum_{m,s}\left\{\gamma^{pdr}_{m,s}\sum_{h\in\Psi_H}P^{DR}_{m,h,s}+\gamma^{hdr}_{m,s}\sum_{h\in\Psi_H}H^{DR}_{m,h,s}\right\}$$

Subject to:

Constraints (2)–(10), (23)–(28), (31), (34), (36), (39) (46)

$$P^{C}_{m,h,s}, Q^{C}_{m,h,s} \in \left[0, \overline{S}^{C}_{m}\right] \quad \forall m,h,s \tag{47}$$

$$tes_{m,h}, ees_{m,h} \in \{0,1\} \quad \forall m,h \tag{48}$$

$$H^{ch}_{m,h,s} \in Eq.(32) \quad \forall m,h,s \tag{49}$$

$$H^{dch}_{m,h,s} \in Eq.(33) \quad \forall m,h,s \tag{50}$$

$$P^{ch}_{m,h,s} \in Eq.(37) \quad \forall m,h,s \tag{51}$$

$$P^{dch}_{m,h,s} \in Eq.(38) \quad \forall m,h,s \tag{52}$$

$$P^{DR}_{m,h,s} \in Eq.(41) \quad \forall m,h,s \tag{53}$$

$$H^{DR}_{m,h,s} \in Eq.(43) \quad \forall m,h,s \tag{54}$$

$$P^{NS}_{e,h,s} \in Eq.(20) \quad \forall e,h,s \tag{55}$$

$$G^{NS}_{g,h,s} \in Eq.(21) \quad \forall g,h,s \tag{56}$$

$$H^{NS}_{t,h,s} \in Eq.(22) \quad \forall t,h,s \tag{57}$$

$$\mu \geq 0,\ \gamma \in (-\infty, +\infty) \quad \forall e,g,t,m,h,s \tag{58}$$

Noted that in Eq. (47), vector of μ includes variables of $\overline{\mu}^{v}_{e,h,s}$, $\underline{\mu}^{v}_{e,h,s}$, $\overline{\mu}^{\rho}_{g,h,s}$, $\underline{\mu}^{\rho}_{g,h,s}$, $\overline{\mu}^{gs}_{g,h,s}$, $\underline{\mu}^{gs}_{g,h,s}$, $\overline{\mu}^{gl}_{g,j,h,s}$, $\underline{\mu}^{gl}_{g,j,h,s}$, $\overline{\mu}^{\tau}_{t,h,s}$, $\underline{\mu}^{\tau}_{t,h,s}$, $\overline{\mu}^{hs}_{t,h,s}$, $\underline{\mu}^{hs}_{t,h,s}$, $\overline{\mu}^{hl}_{t,j,h,s}$, $\underline{\mu}^{hl}_{t,j,h,s}$, $\overline{\mu}^{hc}_{m,h,s}$, $\underline{\mu}^{hc}_{m,h,s}$, $\overline{\mu}^{he}_{m,h,s}$, $\underline{\mu}^{he}_{m,h,s}$, $\overline{\mu}^{ee}_{m,h,s}$, $\underline{\mu}^{ee}_{m,h,s}$, $\overline{\mu}^{ds}_{e,h,s}$, $\overline{\mu}^{el}_{e,j,h,s}$ and $\overline{\mu}^{sc}_{m,h,s}$. These variables refer to Lagrangian multipliers of upper and down limits for voltage, (11), gas pressure, (14), gas station power, (15), gas power of pipeline, (16), temperature, (17), heat station power, (18), heat power of pipeline, (19), heat power of CHP, (30), heat stored energy, (35), and electricity sored energy, (40), constraints (12), (13) and (29). Vector γ contains variables $\gamma^{pdr}_{m,s}$ and $\gamma^{hdr}_{m,s}$that are introduced the Lagrangian multipliers of constraints (42) and (44).

Table Algorithm 1 expresses the process of TLBO + CSA for solving the proposed problem. It is noteworthy that to solve the problem described by (45)-(58), initially, the TLBO + CSA determines N (population size) random values for decision variables based on the constraints (47)–(58). Then, the dependent variables and the fitness function are calculated from constraint (46) and Eq. (45) for each population, respectively. In the following, the steps of updating the decision variables are determined based on the best value of the fitness function of the previous step. In the decision variable updating phase, first the teacher phase, then the student phase, and finally the CSA are implemented. It is assumed that the convergence conditions are available after a specified maximum number of iterations or $iter_{max}$.

Algorithm 1
TLBO + CSA process for problem (45)-(58)

Initialization step
Generation N random values for decision variables based on (47)-(58)
Calculate dependent variables based on constraint (46) that is solved by the Newton-Raphson method
Calculate the fitness function, (45).
Update d**ecision variables**
for i = 1: $iter_{max}$
  Step 1: Run the teacher phase of TLBO to obtain new positions of decision variables according to limits (47)–(58) and the best value of the fitness function of the previous step
  Step 2: Calculate dependent variables and the fitness function
  Step 3: Run Steps 1–2 for the student phase of TLBO based on the best value of the fitness function in Step 2
  Step 4: Run Steps 1–2 for CSA based on the best value of the fitness function in Step 3
End

Algorithm 2. Pseudocode of the TLBO + CSA algorithm for solving of the proposed problem.

4. Numerical results

4.1. Case study

The proposed scheme in this section is implemented in the case study system shown in Fig. 2 [8], which consists of a 9-bus electrical network, a 4-node natural gas network, and a 7-node district heating system. The base power, voltage, pressure, and temperature are 1 MW, 1 kV, 10 bar, 100 °C, respectively. The upper and lower boundaries of voltages, pressures, and temperatures are 1.1 p.u. and 0.9 p.u., respectively [8]. The characteristics of distribution lines and pipelines and peak heat and electrical load data are presented in Ref. [8]. Also, the daily load curve in different places of energy networks is equal to the product of the peak load of that place and the daily load factor curve, which is plotted for electrical and heating networks in Fig. 3(a) [8]. Note that, in this section, it is assumed that CHPs in EHs are the only consumers of gas energy; therefore, the amount of passive gas load is considered to be zero. The price of energy in different networks is also presented in Fig. 3(b) [8], and FOR in the equipment of this network is set at 1%. To achieve high reliability and flexibility for power networks, VOLL and VOLF both are set at 1000 $/MWh. The system under study has 7 EHs whose position in the power network is shown in Fig. 2. Characteristics of sources and ALs of each EH are presented in Table 2. The daily power curve of RESs such as wind system (WS) and photovoltaic (PV) is equal to the product of its capacity and the daily power generation rate curve, which is plotted in Fig. 3(a) [40]. Finally, in the section, the standard deviation of the proposed uncertainty parameters is 10%. To model them, RWM generates 1000 scenarios and then the Kantorovich method selects 20 of them with a high probability of occurrence.

4.2. Results

The proposed FRO scheme for the grid-connected EHs is coded in MATLAB software environment, and then the numerical results from the various case studies are presented as follows.

A) *Capability of the proposed solver*: This section provides the results of the proposed energy management plan using various evolutionary algorithms (EAs) such as grey wolf optimization (GWO) [41], krill herd optimization (KHO) [42], TLBO, CSA, and the TLBO + CSA algorithm. The population size and the maximum number of iterations for all the mentioned algorithms are set 50 and 2000, respectively, and the other adjustment parameters of these solvers are selected according to Refs. [36,37,41,42]. Also, the results obtained by different mathematical algorithms, such as BARON, BONMIN, DISOPT, and KNITO [43] are evaluated for the suggested scheme. Toolbox of these algorithms is available in the GAMS optimization software [43]; hence, the model (1)–(44) is coded in GAMS to solve the problem using these solvers. Additionally, to calculate statistical indices such as the standard deviation of the objective function (1), the general process of each algorithm is repeated 20 times. Finally, the results of this section are presented in Table 3 and Fig. 4.

Based on Table 3, among the mentioned mathematical algorithms, DISOPT and KNITRO cannot find a feasible solution for the proposed scheme. Moreover, between the other two mathematical algorithms, BONMIN solver achieves a more desirable optimal solution than BARON. The reason is that the value of the objective function obtained by BONMIN is less than that found by BARON. Moreover, based on Table 3 and Fig. 4, it can be seen that the TLBO + CSA algorithm has the lowest point or the best solution in the last convergence iteration (2000th iteration) compared to the other mentioned EAs. Also, according to Fig. 4, the convergence speed of this algorithm is high, so that it was able to achieve the convergence point in the 990th iteration and in computational time of 273.3 s according to Table 3. However, these values for other EAs are greater than 1400 iterations and 300 s, respectively. Alternatively, the TLBO + CSA algorithm has a standard deviation of 0.91%, which is the minimum value compared to other GWO, KHO, CSA, and TLBO solvers. This means that the final dispersion in the response of the proposed algorithm is very low, so it has an almost unique response. Finally, according to the obtained results, the

hybrid TLBO-CSA algorithm has a high convergence speed, fewer number of iterations, low computational time, and unique response conditions with respect to other EAs. Comparing the results obtained by TLBO + CSA with mathematical algorithms (BARON and BONMIN), it can be seen that the TLBO + CSA solver has been able to obtain a smaller fitness function than mathematical methods. Although mathematical algorithms converge in fewer iterations than TLBO + CSA, their computational time is longer than the computational time in TLBO + CSA. In terms of the standard deviation of the final response, the mentioned solvers have the same conditions according to Table 3. Therefore, considering these conditions, TLBO + CSA is in a better position than other mathematical algorithms and EAs. These cases are due to the higher number of steps required for updating the decision variables compared to other solvers that are used in Refs. [11,13–15], which is in line with the third contribution of this paper presented in Section 1. In other words, from the perspective of energy networks' operator who needs to achieve optimal planning for available sources and active loads, the use of HEA can be considered as a novelty because, if this algorithm is adopted in the network operator section, it ensures that an accurate and fast solution will be obtained as listed in Table 3 and shown in Fig. 4. In the end, it should be said that the proposed approach has no limitation on executing on larger test systems, but in this case, the population size and the maximum number of convergence iterations of the TLBO-CSA need to be increased as well.

Note that the proposed problem is non-convex, for which most solvers find a locally optimal solution. Among these solvers, the one that finds the most optimal point is more desirable. For instance, the TLBO + CSA algorithm in the proposed scheme can find the most optimal point with respect to TLBO, CSA, GWO and KHO. So, it can be stated that it succeeds to achieve an optimal point close to the optimal global point compared to other mentioned algorithms. In addition, the proposed algorithm provides a lower standard deviation than other algorithms. As a result, it is more capable of other solvers in achieving a rather unique solution. In general, a solver with the most optimal point, higher convergence speed, less dispersion in the response is more suitable for solving nonlinear problems. Among the mentioned algorithms, the TLBO + CSA algorithm is superior to NHEAs for the suggested scheme. This is because of updating decision-making variables in different processes, where the mentioned conditions can also hold for a combination of other algorithms as well.

B) *Performance evaluation of EHs*: The daily power curve of EHs and their sources and ALs is shown in Fig. 5. Fig. 5(a) depicts the expected daily active power curve of the sum of WSs, PVs, EESs, DRPs (IDRPs), EHs, and loads of the EHs. Referring to this figure, RESs inject the active power equal to their maximum capacity into the network at all hours of the simulation. The reason is that the PVs, according to Fig. 3(a), inject active power equal to 1.5 p.u (with the total capacity of EHs given in Table 2). at 15:00 when its power rate is 1. This is the case at other times, and the same is true for WSs. Concerning the ALs, it is observed that EESs and DRPs perform discharge operations during the hours when the price of electricity is cheaper, i.e., between hours 1:00 and 7:00. In other words, in these hours, they receive active power from the network. At the other hours, EESs inject active power into the electrical network (discharge operation), so that from 17:00 to 22:00 (8:00–16:00 and 23:00–24:00) the discharge power level is high (low). It is noteworthy that EES is an active load, so its performance is commensurate with the improvement of the operation status and the reliability and flexibility of energy networks in accordance with the objective function (1). Hence, to improve the operation condition, they perform charging operations during off-peak hours 1:00–7:00 and discharge operations during off-peak hours 17:00–22:00 to minimize operating costs. They also inject active power into the network at other hours to improve the reliability and flexibility of the network. To improve reliability, local sources and ALs will provide a high percentage of load power [5,23], and FSs should control their active power both in charging and discharging modes to improve the flexibility of an electrical system. As a result, according to these cases, EESs inject active power into the electrical network between 8:00–16:00 and 23:00–24:00. This is true for DRPs, except that they receive active power from the network during that time. The reason is that reducing the high power during peak hours to minimize the objective function (1) requires an increase in power consumption compared to the case before DRP implementation during low-load and middle-load hours, i.e. 1:00–16:00 and 23:00–24:00. In other words, their only charging function during off-peak hours, 1:00–7:00, cannot meet their discharge operation during peak hours, 17:00–22:0. Therefore, they only play a role in improving the flexibility of the electrical system in the middle-load interval with no role in enhancing the reliability of the network due to power consumption. Nonetheless, in general, their performance on the horizon of 24 h is commensurate with the improvement of the reliability, operation, and flexibility of the electrical network. In addition, since the difference between the total prices of electricity and heat compared to the price of gas energy always has a positive value according to Fig. 3(b), the CHPs at all hours of simulation inject high power to the network. As can be seen from Fig. 5(a), they inject more than 2.5 p.u. active power into the electrical network, although the capacity of all CHPs according to Table 3 is 3 p.u. Referring to Eq. (24), the only local source in EH to supply its reactive load is CHP; hence, 0.5 p.u. of the remaining capacity of the CHPs is used to supply the reactive load of EHs. Finally, based on Eq. (23), the active power of EHs will be calculated, which is represented in pink in Fig. 5(a). According to this curve, EHs receive active power from the electrical network from 1:00 to 7:00 due to the high consumption of ALs but can inject active power into the electrical network at other hours.

Fig. 5(b) illustrates the expected daily reactive power curve of all CHPs, EHs and their load. Based on this figure, CHPs produce more reactive power than EHs reactive load during all simulation hours. Therefore, according to Eq. (24), the reactive power of EHs in the 24-h horizon is always positive, so they inject reactive power into the electrical network at all hours. According to Ref. [23], the most important factor in improving the voltage in the electrical network is the optimal injection of reactive power into the electrical network by local sources. Therefore, it is expected that the injection of reactive power of EHs into the network aims to improve the voltage of the network. Moreover, the expected daily heat curve of the sum of CHPs, DRPs, TESs, EHs, and EH loads is shown in Fig. 5(c). Based on this figure, the performance of heat ALs, i.e., TES and DRP, is similar to that of electrical ALs. In other words, during peak heat hours, i.e., 5:00–15:00, which according to Fig. 3(b) is proportional to the high price of heat energy, they inject heat power into the district heating network. And, during off-peak hours, 16:00–24:00 with low heat energy price, receive heat power from the district heating network. TESs also perform discharge operations from 1:00 to 4:00, but DRPs perform charging operations. In general, this operation mode of heat ALs is similar to electrical ALs to improve the operation, reliability, and flexibility of the district heating

network. It is worth noting that the heat power of CHP, as given in Eq. (27), is a factor of its active power, so the daily heat power curve of CHPs in Fig. 5(c) is the same as the daily curve of the active power of CHPs shown in Fig. 5(a), which differ only in number. Finally, the heat power of EHs is calculated based on Eq. (25), which is represented in pink in Fig. 5(c). According to this curve, EHs can inject heat into the district heating network from 1:00 to 15:00, but they are heat consumers at other times.

The expected daily gas power curve of the CHPs and EHs is plotted in Fig. 5(d). According to Eq. (26), the gas power of EHs is equal to the gas power consumption of CHPs, so their curves will be symmetrical with each other in all simulation hours as in Fig. 5(d). Also, the gas power of CHPs is a factor of their active power based on Eq. (28). Hence, their gas power curve is the same as their active power, which differs only numerically.

C) *Evaluation of technical and economic indices in energy networks*: In this section, numerical results are extracted for the following two case studies:
- **Case I:** Power flow studies of energy networks, i.e., only considering Eqs. (2)–(10) by removing the EH variables
- **Case II:** Considering the proposed scheme with the problem model described by (1)-(44)

The problem presented in Case I is solved using the Newton-Raphson numerical method, but the proposed problem in Case II will be solved using the hybrid TLBO and CSA algorithm. The economic and operation results of electricity, natural gas, and district heating networks in the presence of the EHs are tabulated in Table 4. According to this table, Case I is related merely to energy costs in heating and electrical networks, and the operating cost of the natural gas network, in this case, is zero because only EHs were considered as the consumers of the natural gas network in this study, their presence is which is not focused in this case study. Under these circumstances, the total energy cost is $ 4323.8. However, in Case II, with the energy cost of $ 1425.4 for the natural gas network, the energy costs of electricity and heating networks are reduced by about $ 983 (2081.8−1098.8) and $ 1118.8 (22411−122.2), respectively, compared to Case I. In these conditions, the total energy cost is $ 3646.4, which is about 15.7% ((4323.8−3646.4)/4323.8) less than in Case I. Therefore, the optimal performance of EHs, as shown in Fig. 5, can improve the economic status of energy networks. In addition, in Case I, the energy loss, pressure drop, or overpressure in the natural gas network due to the absence of the consumer is zero. Nonetheless, in these conditions, energy loss in electrical and heating networks is 2.3284 p.u. and 2.5036 p.u., respectively. Also, the voltage and temperature drops are 0.157 p.u. and 195 p.u., respectively, which are less than their allowable limit of 0.1 p.u. Hence, according to Table 4, Case I is not in a feasible condition due to the violation of temperature and voltage limits. However, in Case II, by energy management of the EHs following Fig. 5, the proposed scheme has been able to reduce the temperature and voltage drop to less than 0.1 p.u., which is proportional to overheating of about 0.012 p.u. (less than the allowable overheating of 0.1 p.u.) and a pressure drop of about 0.063 p.u. (less than the allowable pressure drop of 0.1 p.u.). Therefore, Case II does not violate its solution space, and also succeeds to reduce the total energy loss in the system of Fig. 2 by about 15.8% ((4.832−4.069)/4.832) compared to Case I by creating an energy loss of 1.1381 p.u. in the natural gas network.

Fig. 6 displays the reliability indices curves, i.e. EENS, reliability cost, and the expected operating cost of energy networks in terms of the VOLL penalty price. Based on this figure, with increasing VOLL, EENS decreases, reliability cost for VOLL increases between zero and 10 $/MWh and decreases for other VOLL values and operating cost increases. In the end, high reliability is achieved for power grids when VOLL equals 60 $/MWh so that EENS and the reliability cost in such conditions are zero. However, such conditions are commensurate with the high operating cost relative to lower VOLL values of 60 $/MWh. Moreover, the curves of flexibility indices such as EFE, flexibility cost, and operating cost of energy networks in terms of VOLF penalty price are plotted in Fig. 7. As given in Fig. 7, increasing VOLF reduces EFE and increases operating costs. Yet, its increase in the range of zero to 2 $/MWh leads to the increase in the flexibility cost, while in other values of VOLF, this is reversed. For a VOLF equal to 50 $/MWh, EFE and flexibility cost are zero, which means high flexibility of energy networks and EHs. Nevertheless, these conditions are commensurate with the high operating cost compared to VOLFs less than 50 $/MWh. Finally, based on Figs. 6 and 7, enhancing the reliability and flexibility in a system corresponds to the high operating cost.

In comparing the proposed scheme with the literature [7–22] that discard flexibility and reliability model (equivalent to VOLL = 0 and VOLF = 0), it is observed that the models in the literature cannot confront consumer interruption in case of an N - 1 event, as shown in Fig. 6(a). Also, referring to Fig. 7(a), there will be significant EFE for EHs in case their operation model is based on the model proposed in Refs. [7–22]. Therefore, they are expected to show very low flexibility in EHs, resulting in the unbalance of supply and demand in real-time operation [3]. Nonetheless, by considering the penalty price of VOLL and VOLF for EHs and increasing the operating cost, the proposed scheme can resolve the abovementioned challenges. Note that the operating cost in the proposed scheme increase by about 10.6% and 7.35% compared to the schemes presented in Refs. [7–22], as illustrated in Fig. 6(c) and Fig. 7(c). However, it can achieve higher reliability/flexibility in EHs by spending this cost.

D) *Investigation of the capability of the proposed scheme in a large-scale test system*: In this section, in order to evaluate the capabilities of the proposed scheme in larger networks, the numerical results of applying the proposed problem to the large-scale test system as in Fig. 8 are evaluated. This system consists of three systems, Fig. 2, that are connected to a gas station (i.e. all three nodes on the right side in Fig. 8 represent the g1 node in Fig. 2). Therefore, various data such as load, energy price and energy hubs follow subsection 4.1. Also, in this section, population size and maximum number of convergence iterations for EAs are considered to be 50 and 4000, respectively.

The technical, economic and convergence results of this section are summarized in Table 5. Based on this table, it can be seen that in this case study, the TLBO + CSA algorithm is able to obtain a more optimal solution than mathematical solvers and NHEAs so that the minimum value of the objective function is obtained by it at a lower computational time. Also, in this section, although the volume of the problem has increased, the standard deviation of the final response of the TLBO + CSA algorithm is around 0.9% and is close to the results presented in Table 3, while this is not the case in NHEAs. This suggests that the response dispersion of the algorithm has very low dependence on the volume of the problem, which can be another advantage for the suggested solver. In addition, as in subsection 4.2.C, the proposed EH energy management scheme has been able to reduce the operating cost of energy networks compared to power flow studies. This also applies to the operation indices of energy networks so that the energy losses in the proposed plan are reduced compared to power flow studies. Also, smoother voltage and temperature profiles (because of low voltage deviation) for energy networks have been obtained based on the

proposed design compared to power flow studies. Of course, these results are proportional to the increase in overheating and pressure drop, but their amount is less than the allowable limit of 0.1 p.u. By adopting a penalty price of 100 $/MWh for reliability and flexibility, i.e. VOLL = VOLF = 100 $/MWh, the scheme has achieved EFE and EENS equal to zero. Therefore, the mentioned plan, similar to subsection 4.2.C, can achieve high reliability for energy networks by adopting the desirable penalty price, and besides, EHs are present in the mentioned networks with high flexibility.

5. Conclusion

This paper describes the FRO optimization model for electrical, natural gas, and district heating networks in the presence of the EHs. EH includes ESS and DRP to adjust its flexibility in the presence of RES and CHP. Therefore, in the suggested scheme, this issue is to minimize the total expected operating costs, reliability, and flexibility of the mentioned networks, which is constrained to the OPF equations and the reliability constraints of energy networks, and the EH model in the presence of power sources and ALs. This problem utilizes the MINLP model. In this paper, the hybrid TLBO and CSA algorithm is used to achieve an optimal solution. Also, the SBSP method based on the combined RWM and Kantorovich method is employed to model uncertainties of the load, energy price, power generation of RESs, and availability of energy network equipment. Finally, based on the numerical results of various studies, it is observed that the proposed hybrid EA can provide the optimal solution with a standard deviation of 0.91%, the optimal value of the objective function in the least number of convergence iterations, and low computational time compared to non-hybrid evolutionary algorithms. Additionally, to improve the operation, reliability, and flexibility of energy networks, ALs in EHs generally perform charging and discharging operations during off-peak and peak hours. ESSs and DRPs perform discharging and charging during middle-load hours, respectively. Also, to enhance the operation and reliability of these networks, RES, and CHPs operate at their maximum electrical capacity point. Following the optimal performance of resources and ALs in EHs in accordance with the proposed energy management scheme, the economic conditions of energy networks are improved by about 15.7% compared to power flow studies. In terms of operation, energy loss is improved by about 15.8% compared to power flow studies, and the voltage profile, pressure, and temperature are smoother, as the proposed scheme can decrease deviations of the variables relative to 1 p.u.

Credit author statement

Anoosh Dini: Conceptualization; Data curation; Formal analysis; Funding acquisition; Investigation; Methodology; Project administration; Resources; Software; Supervision; Validation; Visualization; Roles/Writing - original draft; Writing – review & editing. Alireza Hassankashi: Conceptualization; Data curation; Formal analysis; Funding acquisition; Investigation; Methodology; Project administration; Resources; Software; Supervision; Validation; Visualization; Roles/Writing - original draft; Writing – review & editing. Sasan Pirouzi: Conceptualization; Data curation; Formal analysis; Investigation; Methodology; Project administration; Resources; Supervision; Validation; Visualization; Roles/Writing - original draft; Writing – review & editing. Matti Lehtonen: Writing – review & editing. Ali Asghar Baziar: Writing – review & editing.

Declaration of competing interest

The authors declare that they have no known competing financial interests or personal relationships that could have appeared to influence the work reported in this paper.

References

[1] Nosratabadi SM, Jahandide M, Khajoei Nejad R. Simultaneous planning of energy carriers by employing efficient storages within main and auxiliary energy hubs via a comprehensive MILP modeling in distribution network. Journal of Energy Storage 2020;30:101585.

[2] Karkhaneh J, Allahvirdizadeh Y, Shayanfar H, Galvani S. Risk-constrained probabilistic optimal scheduling of FCPP-CHP based energy hub considering demand-side resources. Int J Hydrogen Energy 2020;45:16751–72.

[3] Bozorgavari SA, Aghaei J, Pirouzi S, Vahidinasab V, Farahmand H, Korpås M. Two-stage hybrid stochastic/robust optimal coordination of distributed battery storage planning and flexible energy management in smart distribution network. Journal of Energy Storage 2020;26:100970.

[4] Nazari-Heris M, Mohammadi-Ivatloo B, Gharehpetian GB, Shahidehpour M. Robust short-term scheduling of integrated heat and power microgrids. IEEE Systems Journal Sept. 2019;13(3):3295–303.

[5] Dini A, et al. Hybrid stochastic/robust scheduling of the grid-connected microgrid based on the linear coordinated power management strategy. Sustainable Energy, Grids and Networks 2020;24:100400.

[6] Jannati M, Foroutan E, Mousavi SMS, Grijalva S. An intelligent energy management system to use parking lots as energy storage systems in smoothing short-term power fluctuations of renewable resources. Journal of Energy Storage 2020;32:101905.

[7] Zafarani HR, Taher SA, Shahidehpour M. Robust operation of a multicarrier energy system considering EVs and CHP units. Energy 2020;192:1–12.

[8] Dini A, Pirouzi S, Norouzi MA, Lehtonen M. Grid-connected energy hubs in the coordinated multi-energy management based on day-ahead market framework. Energy 2019;188:116055.

[9] Afrashi K, Bahmani-Firouzi B, Nafar M. Multicarrier energy system management as mixed integer linear programming. Iranian Journal of Science and Technology, Transactions of Electrical Engineering 2020;PP:1–13.

[10] Afrashi K, Bahmani-Firouzi B, Nafar M. IGDT-based robust optimization for multicarrier energy system management. Iranian Journal of Science and Technology, Transactions of Electrical Engineering 2020;PP:1–13.

[11] Eladl AA, El-Afifi MI, Saeed MA, El-Saadawi MM. Optimal operation of energy hubs integrated with renewable energy sources and storage devices considering CO2 emissions. Int J Electr Power Energy Syst 2020;117:105719.

[12] Cao Y, Wei W, Wang J, Mei S, Shafie-khah M, Catalão JPS. Capacity planning of energy hub in multi-carrier energy networks: a data-driven robust stochastic programming approach. IEEE Transactions on Sustainable Energy Jan. 2020;11(1):3–14.

[13] Derafshi Beigvanda S, Abdia H, La Scalab M. Economic dispatch of multiple energy carriers. Energy 2017;138:861–72.

[14] Shabanpour-Haghighi A, Seifi AR. Energy flow optimization in multicarrier systems. IEEE Transactions on Industrial Informatics 2015;11:1067–77.

[15] Derafshi Beigvanda S, Abdia H, La Scalab M. A general model for energy hub economic dispatch. Appl Energy 2017;190:1090–111.

[16] Majidi M, Zare K. Integration of smart energy hubs in distribution networks under uncertainties and demand response concept. IEEE Trans Power Syst Jan. 2019;34(1):566–74.

[17] Alipour M, Zare K, Abapour M. MINLP probabilistic scheduling model for demand response programs integrated energy hubs. IEEE Transactions on Industrial Informatics Jan. 2018;14(1):79–88.

[18] Zhao P, et al. Economic-effective multi-energy management considering voltage regulation networked with energy hubs. IEEE Trans Power Syst May 2021;36(3):2503–15.

[19] Zhao N, Wang B, Bai L, Li F. Quantitative model of the electricity-shifting curve in an energy hub based on aggregated utility curve of multi-energy demands. IEEE Transactions on Smart Grid March 2021;12(2):1329–45.

[20] Zhao N, Wang B, Li F, Shi Q. Optimal energy-hub planning based on dimension reduction and variable-sized unimodal searching. IEEE Transactions on Smart Grid March 2021;12(2):1481–95.

[21] Jadidbonab M, Mohammadi-Ivatloo B, Marzband M, Siano P. Short-term self-scheduling of virtual energy hub plant within thermal energy market. IEEE Trans Ind Electron April 2021;68(4):3124–36.

[22] Liu Z, Zeng M, Zhou H, Gao J. A planning method of regional integrated energy system based on the energy hub zoning model. IEEE Access 2021;9:32161–70.

[23] Hamidpour HR, Aghaei J, Dehghan S, Pirouzi S, Niknam T. Integrated resource expansion planning of wind integrated power systems considering demand response programmes. IET Renew Power Gener 2018;13(4):519–29.

[24] Shahbazi A, et al. Hybrid stochastic/robust optimization model for resilient architecture of distribution networks against extreme weather conditions. Int J Electr Power Energy Syst 2021;126:106576.

[25] Pirouzi S, Latify MA, Yousefi GR. Conjugate active and reactive power management in a smart distribution network through electric vehicles: a mixed integer-linear programming model. Sustainable Energy, Grids and Networks 2020;22:100344.

[26] Kiani H, Hesami K, Azarhooshang AR, Pirouzi S, Safaee S. Adaptive robust operation of the active distribution network including renewable and flexible sources. Sustainable Energy, Grids and Networks 2021;26:100476.

[27] Pirouzi S, Aghaei J. Mathematical modeling of electric vehicles contributions

in voltage security of smart distribution networks. Simulation: Transactions of the Society for Modeling and Simulation International 2018;95(5):429–39.
[28] Shahbazi A, Aghaei J, Pirouzi S, Niknam T, Shafie-khah MR, Catalão JPS. Effects of resilience-oriented design on distribution networks operation planning. Elec Power Syst Res 2021;191:106902.
[29] Norouzi MA, Aghaei J, Pirouzi S, Niknam T, Lehtonen M. "Flexible operation of grid-connected microgrid using ES," *IET Generation*. Transm Distrib 2019;14(2):254–64.
[30] Bozorgavari SA, Aghaei J, Pirouzi S, Nikoobakht A, Farahmand H, Korpås M. Robust planning of distributed battery energy storage systems in flexible smart distribution networks: a comprehensive study. Renew Sustain Energy Rev 2020;123:109739.
[31] Aghaei J, Bozorgavari SA, Pirouzi S, Farahmand H, Korpås M. Flexibility planning of distributed battery energy storage systems in smart distribution networks. Iranian Journal of Science and Technology, Transactions of Electrical Engineering 2019;44(3):1105–21.
[32] Kavousi-Fard A, Khodaei A. Efficient integration of plug-in electric vehicles via reconfigurable microgrids. Energy 2016;111:653–63.
[33] Amirioun MH, Kazemi A. A new model based on optimal scheduling of combined energy exchange modes for aggregation of electric vehicles in a residential complex. Energy 2014;69:186–98.
[34] Aghaei J, Amjady N, Baharvandi A, Akbari MA. "Generation and transmission expansion planning: MILP–based probabilistic model. *IEEE Trans* Power Syst 2014;29(4):1592–601.
[35] Aghaei J, Barani M, Shafie-khah M, Nieta AASdl, Catalão JPS. Risk-constrained offering strategy for aggregated hybrid power plant including wind power producer and demand response provider. IEEE Transactions on Sustainable Energy 2016;7(2):513–25.
[36] Gill HS, Khehra BS, Singh A, Kaur L. Teaching-learning-based optimization algorithm to minimize cross entropy for Selecting multilevel threshold values. Egyptian Informatics Journal 2019;20:11–25.
[37] Askarzadeh A. A novel metaheuristic method for solving constrained engineering optimization problems: crow search algorithm. Comput Struct 2016;169:1–12.
[38] Katoch S, Chauhan SS, Kumar V. A review on genetic algorithm: past, present, and future. Multimed Tool Appl 2021;80:8091–126.
[39] Najy WKA, Zeineldin HH, Woon WL. Optimal protection coordination for microgrids with grid-connected and islanded capability. IEEE Trans Ind Electron April 2013;60(4):1668–77.
[40] Maleki A, Askarzadeh A. Optimal sizing of a PV/wind/diesel system with battery storage for electrification to an off-grid remote region: a case study of Rafsanjan, Iran. Sustainable Energy Technologies and Assessments 2014;7:147–53.
[41] Mirjalili SA, Mirjalili SM, Lewis A. Grey wolf optimizer. Adv Eng Software 2014;69:46–61.
[42] Rani RR, Ramyachitra D. Krill herd optimization algorithm for cancer feature selection and random forest technique for classification. Beijing: IEEE International Conference on Software Engineering and Service Science (ICSESS); 2017. p. 109–13.
[43] Generalized algebraic modeling systems (GAMS) [Online]. Available: http://www.gams.com.